Human Pathology (2019) **85**, 174–183

ELSEVIER

Human PATHOLOGY

www.elsevier.com/locate/humpath

Original contribution

Spindle assembly checkpoint MAD2 and CDC20 overexpressions and cell-in-cell formation in gastric cancer and its precursor lesions☆,☆☆

Younghye Kim MD, PhD, Jung-Woo Choi MD, PhD, Ju-Han Lee MD, PhD, Young-Sik Kim MD, PhD*

Department of Pathology, Korea University Ansan Hospital, Ansan, 15355 Republic of Korea
Department of Pathology, College of Medicine, Seoul, 02841 Republic of Korea

Received 27 July 2018; revised 24 October 2018; accepted 31 October 2018

Keywords:
MAD2;
CDC20;
Cell-in-cell structure;
Aneuploidy;
Gastric cancer

Summary Overexpression of mitotic arrest deficient 2 (MAD2) and/or cell division cycle 20 (CDC20) in the spindle assembly checkpoint leads to chromosomal instability and aneuploidy. Cell-in-cell (CIC) structures are formed by the process where cancer or immune cells are internalized into adjacent host cancer cells. Here, we investigated the clinicopathological significances of spindle assembly checkpoint protein overexpression and CIC structures in 829 cases of normal, premalignant, and gastric cancer (GC) lesions. MAD2 and CDC20 expressions were significantly increased in intestinal metaplasia, low-grade dysplasia, high-grade dysplasia (HGD), and early GC than normal mucosa, and their expression levels were the highest in HGD. Interestingly, CDC20 immunohistochemistry specifically stained the outer cells of CIC structures, which were the most frequently observed in early GC. In univariate analyses, MAD2 and CDC20 overexpressions and CIC formation were associated with older age, intestinal histology, lower tumor-node-metastasis stage, and longer recurrence-free survival and cancer-specific survival of GC patients. In multivariate survival analyses, MAD2 and CDC20 overexpressions were associated with better recurrence-free survival (hazard ratio, 0.61; $P = .012$) and cancer-specific survival (hazard ratio, 0.63; $P = .043$), respectively. In conclusion, MAD2 and CDC20 are the most expressed in HGD, suggesting their roles in the early stage of gastric carcinogenesis, whereas their overexpressions in GC are associated with intestinal histology and favorable clinicopathological parameters, which may be useful for immunohistochemical classification of chromosomal instability–type GC. Moreover, CDC20 is a novel immunohistochemical marker for highlighting CIC structures.
© 2018 Elsevier Inc. All rights reserved.

☆ Competing interests: The authors declare no competing interests.
☆☆ Funding/Support: This work was supported by Mid-career Researcher Program through a National Research Foundation of Korea grant (Grant No. 2016 R1A2B4012030) funded by the Ministry of Education, Science and Technology.
* Corresponding author at: Department of Pathology, Korea University Ansan Hospital, 123, Jeokgeum-Ro, Danwon-Gu, Ansan-Si, Gyeonggi-Do 15355, Republic of Korea.
E-mail address: apysk@korea.ac.kr (Y. -S. Kim).

https://doi.org/10.1016/j.humpath.2018.10.029
0046-8177/© 2018 Elsevier Inc. All rights reserved.

1. Introduction

Gastric cancer (GC) is the fifth most common cancer worldwide and the third leading cause of cancer death in developed countries in 2013 [1]. Most GCs are considered to occur through a gradual process of atrophic gastritis, intestinal metaplasia (IM), low-grade dysplasia (LGD), and high-grade dysplasia (HGD) [2]. A major event in intestinal type gastric carcinogenesis is chromosomal instability (CIN), which is defined as a high rate of chromatin missegregation involving loss of heterozygosity, gene amplifications, mutations, and rearrangements. CIN can lead to DNA aneuploidy, so-called a state of improper numbers of chromosomes and a hallmark of cancer, through dysregulated spindle assembly checkpoint (SAC) [3].

Chromosomal segregation is tightly controlled by SAC, which is a surveillance mechanism for chromosomal stability. Dysregulation of SAC could lead to chromosome missegregation and consequently aneuploidy, contributing to cancer development. Unattached kinetochores promote the formation of the mitotic checkpoint complex consisting of budding uninhibited by benzimidazoles (Bub) R1, Bub3, mitotic arrest deficient (MAD) 2, and cell division cycle 20 (CDC20), which inhibits the anaphase-promoting complex or cyclosome (APC/C) during the early phase of mitosis [4,5]. When mitotic spindles are correctly attached to all kinetochores, the mitotic checkpoint complex is not formed and free CDC20 activates APC/C, finally leading to the metaphase-anaphase transition and mitotic exit by degrading securin and cyclin B1. Several lines of evidence have shown that MAD2-CDC20 binding is the most important step in the correct functioning of SAC [6].

More recently, comprehensive molecular profiling using The Cancer Genome Atlas has proposed 4 molecular subtypes of gastric adenocarcinoma, including Epstein-Barr virus–associated, microsatellite instable, CIN, and genomically stable types [7]. Among these, the most frequent subtype is CIN group, which is characterized by intestinal histology, a high frequency of aneuploidy, and *TP53* mutations [7]. *TP53* mutations and Rb-E2F pathway deregulation induce the overexpression of MAD2 and CDC20 [8-10], which is more important in cancer development rather than gene mutations, because mutations in the MAD2 and CDC20 genes are rarely found in human tumors [11]. Overexpression of MAD2 and CDC20 proteins has been reported in a variety of tumors, including GC [12-16]. However, little is known about the clinicopathological significance of SAC protein overexpression from the standpoint of gastric carcinogenesis.

Cell-in-cell (CIC) structures are formed by the process of cell cannibalism, entosis, and emperitosis, in which cancer or immune cells are internalized into adjacent host cancer cells [17,18]. Cell cannibalism is the process where host cancer cells that are starved to death or in an acidic microenvironment nonselectively swallow the nearby cancer or immune cells and eventually absorb nutrients from the internalized cells to exploit cellular proliferation [18]. Entosis is a nonapoptotic lysosome-mediated death, in which a cancer cell invades the surrounding cancer cells, or when cancer cells detached from the matrix or matrix-adhering cancer cells in an abnormal mitosis state or with starvation and low AMP-activated protein kinase levels are internalized into adjacent cancer cells [18]. Emperitosis refers to the phenomenon where immune killer cells including natural killer cells and CD8+ cytotoxic T lymphocytes invade cancer cells and granzyme B secreted by the cytotoxic T lymphocyte itself is not transferred to the host cell in the vacuole but reuptakes itself to death by apoptosis [18]. Like the overexpression of SAC proteins, CIC formation can induce CIN and aneuploidy in host cancer cells by the process of cytokinesis failure, cell fusion, or direct exchange of genetic material [19].

Thus, to determine the clinicopathological significances of SAC protein overexpression and formation of CIC structures in gastric carcinogenesis, we investigated (1) the frequency of MAD2 and CDC20 overexpressions and CIC formation at each stage of GC development, (2) whether MAD2 or CDC20 was expressed in the CIC structures, and (3) whether the SAC protein overexpression and CIC formation were associated with the clinicopathological factors of GC.

2. Materials and methods

2.1. Patients and tissue samples

We studied 829 cases including 21 cases of normal gastric mucosa, IM 50 cases, LGD 50 cases, HGD 50 cases, early GC (EGC) 345, cases and advanced GC (AGC) 313 cases. The samples were collected in 2002 to 2010 and were archived in the Department of Pathology, Korea University Ansan Hospital. The specimens were fixed in 10% buffered formalin, embedded in paraffin, and stained with hematoxylin and eosin for histologic assessment. The median age of patients was 62 years (range, 19-86 years): 69 years (range, 39-76 years) for normal mucosa, 67 years (range, 42-80 years) for IM, 67 years (range, 39-79 years) for LGD, 67 years (range, 39-84 years) for HGD, 61 years (range, 19-85 years) for EGC, and 61 years (range, 26-86 years) for AGC. All cases were reviewed for clinicopathological parameters, including histologic grade, tumor-node-metastasis (TNM) stage, the presence or absence of lymphatic or perineural tumor invasion, tumor recurrence, and distant metastasis. When the diffuse component accounts for more than 10% of all tumors, the GC showing the mixed intestinal and diffuse histologic types was classified as diffuse type. The TNM stage was determined in accordance with the guidelines of the American Joint Committee on Cancer, eighth edition, published in 2017 [20]. This study was conducted with the approval of the institutional review board of Korea University Ansan Hospital (No. 2018AS0092).

2.2. Tissue microarray construction

Three representative 1-mm cores were obtained from each case after reviewing all the hematoxylin and eosin-stained slides and inserted in a grid pattern into a recipient paraffin block using

a tissue arrayer (Beecher Instruments, Sun Prairie, WI). Tissue microarray sections were constructed, and the results were interpreted according to the proposed guidelines [21].

2.3. Immunohistochemistry and double immunohistochemistry

Immunohistochemical analysis was performed using the Leica BOND-MAX autostainer and Leica Refine detection kit (Leica Biosystems, Melbourne, Australia). The primary MAD2 (1:50, clone 48/MAD2; BD Transduction Laboratories, San Jose, CA) and CDC20 (1:50, clone E-7; Santa Cruz Biotechnology, Dallas, TX) antibodies were used. Tissue sections were deparaffinized, dehydrated, and heated for 20 minutes using BOND-MAX Epitope Retrieval solution (EDTA buffer, pH 8.0). Endogenous peroxidase activity was quenched by incubation with hydrogen peroxide for 10 minutes. After incubation with primary antibody for 30 minutes, polymer for 15 minutes, and postpolymer for 15 minutes, the sections were treated with 3,3′-diaminobenzidine tetrahydrochloride solution containing hydrogen peroxide and counterstained with hematoxylin. For double immunohistochemistry, the first MAD2 immunostaining was done using the same protocol of the single immunohistochemistry, followed by the second CDC20 immunostaining using the Bond Polymer Refine Red Detection kit.

2.4. Quantitative scoring

Digital images were acquired using an Olympus BX51 light microscope with a DP70 digital camera (Olympus, Tokyo, Japan). Three microscopic images from each tissue microarray core were taken at ×40 magnification and saved in JPEG format at 1360 × 1024-pixel resolution. The percentage of the 3,3′-diaminobenzidine–stained area to the total nuclear area was calculated using ImageJ software (http://rsb.info.nih.gov/ij). For each case, the average percentage of the stained areas of the 3 cores was used. Each cutoff value between high and low expression of MAD2 and CDC20 was determined by the results of receiver operator characteristic curves for tumor invasion depths because they represent the highest area under the curve in receiver operator characteristic analyses [22].

We considered cases as having a high MAD2 expression level if the percentage of MAD2-stained area was >28.8% and a high CDC20 level if the percentage of CDC20-stained area was >6.9% for statistical analysis. Homotypic CIC structures of tumor cells are morphologically defined when cancer cells are internalized into adjacent host cancer cells. In other words, one tumor cell is completely engulfed by another tumor cell, and the internalized cell is housed within a vacuole in the outer host cell cytoplasm. Only homotypic CIC structures formed between tumor cells were counted. The number of CIC structures was counted at three ×40 magnification fields per tissue core. Thus, a total of 9 of CIC formation numbers are obtained from 3 tissue cores per case. The maximal number of these 9 high-power fields was used for statistical analysis as a representative value of CIC formation.

2.5. Statistical analysis

The expression of MAD2 and CDC20 and the number of CIC structures in the gastric normal mucosa, IM, LGD, HGD, and GC were compared using Kruskal-Wallis test with post hoc Mann-Whitney *U* test for each pair of groups. Initially, the Kruskal-Wallis test was used to examine whether there was at least 1 pair with a significant difference when compared with each other in the 6 groups, and then the differences between the 2 groups of each pair were compared using the post hoc Mann-Whitney *U* tests. The correlation between MAD2 and CDC20 expressions was determined by Spearman analysis. The relationship between the presence or absence of

Table 1 MAD2 and CDC20 overexpressions and CIC formation in premalignant and malignant gastric lesions

Group	Case no.	MAD2 (% area)		CDC20 (% area)		CIC structures		
		Mean ± SD	*P*	Mean ± SD	*P*	Case no. with CIC (%)	Mean (range)	*P*
Normal	21	19.94 ± 8.50	Ref	3.42 ± 1.54	Ref	0 (0.0)		
IM [a]	50	40.31 ± 12.02	<.001 *	10.31 ± 3.78	<.001 *	2 (4.0)	1	Ref
LGD [b]	50	40.59 ± 15.46	.975	11.11 ± 4.22	.296	7 (14.0)	1	1.00
HGD [c]	50	48.46 ± 19.75	.064	18.82 ± 8.91	<.001 *	27 (54.0)	1.33 (1-3)	1.00
EGC [d]	345	39.89 ± 18.39	.007 *	10.56 ± 7.67	<.001 *	205 (59.4)	2.49 (1-9)	.013 *
AGC [e]	313	24.64 ± 14.41	<.001 *	5.73 ± 4.14	<.001 *	99 (31.6)	1.67 (1-8)	.008 *

Abbreviation: Ref, reference.
[a] Compared with Normal.
[b] Compared with IM.
[c] Compared with LGD.
[d] Compared with HGD.
[e] Compared with EGC.
* Statistically significant.

CIC structures and clinicopathological characteristics of early and AGCs was analyzed using χ^2 test. Recurrence-free survival (RFS) and cancer-specific survival (CSS) in all GCs according to the high or low expression levels of MAD2 or CDC20 and the presence or absence of CIC structures were compared using Kaplan-Meier curves and log-rank tests. Multivariate survival analyses were performed using the Cox proportional hazards model. Statistical significance was defined as $P < .05$. All statistical analyses were performed with SPSS for Windows 10.0 (SPSS, Chicago, IL).

3. Results

3.1. MAD2 and CDC20 expression

In this study, we compared the expression of MAD2 and CDC20 in each pair of 6 groups, including normal gastric mucosa, IM, LGD, HGD, EGC, and AGC, but presented only the comparisons between normal gastric mucosa and IM, IM and LGD, LGD and HGD, HGD and EGC, and EGC and AGC (Table 1). Both MAD2 and CDC20 expressions were significantly upregulated in IM, LGD, HGD, and EGC, except AGC, compared with normal gastric mucosa. Among these, the highest expression of both proteins was observed in HGD (Fig. 1A and B), and their expression was localized to the nucleus and/or cytoplasm of gastric epithelial, dysplastic, or cancer cells.

MAD2 was expressed mainly at the isthmus of normal tissue, at the base of IM, and in the upper one-third in LGD. MAD2 was randomly expressed in HGD, EGC, and AGC (Supplementary Fig. 1). MAD2 expression was more increased in IM, LGD, HGD, and EGC compared with normal gastric tissue ($P < .001$; Fig. 1A, Supplementary Fig. 1 A-F). MAD2 expression did not show any significant difference between IM, LGD, and HGD, although the average value of the MAD2 expression in HGD was moderately higher than in those of the other groups (IM versus LGD, $P = .975$; LGD versus HGD, $P = .064$). MAD2 expression gradually decreased in EGCs and AGCs compared with HGDs ($P = .007$ and $P < .001$, respectively).

CDC20 expression was similar to the expression patterns of MAD2 and also observed mainly at the isthmus of normal gastric tissue, at the base of IM, and in the upper one-third in LGD. CDC20 was not restricted to one place and appeared without regularity in HGD, EGC, and AGC (Supplementary Fig. 2). CDC20 expression was significantly increased in IM and LGDs than in normal gastric mucosa ($P < .001$), but there was no difference of CDC20 levels between IM and LGD ($P = .296$; Fig. 1B, Supplementary Fig. 2A-F). CDC20 expression was the highest in HGD among the other groups (LGD versus HGD, $P < .001$; HGD versus EGC, $P < .001$). CDC20 expression in EGC was more increased than that of AGC ($P < .001$). Thus, CDC20 expression was decreased in the order of HGD, EGC, and AGC.

MAD2 expression was positively correlated with CDC20 expression in all samples (Spearman $P = 0.719$, $P < .001$). Interestingly, a sudden decrease in the expression of MAD2 and CDC20 was observed in the invasive front of EGC compared with adjacent HGD. (Supplementary Fig. 3A and B).

MAD2 and CDC20 expressions in GC patients were analyzed with clinicopathological parameters (Table 2). High MAD2 and CDC20 expressions were associated with favorable prognostic factors, except for older age group. Overexpression of MAD2 and CDC20 was more frequently observed in male ($P = .001$ and $P = .001$), older age ≥60 years ($P < .001$ and $P < .001$), intestinal histologic type ($P < .001$ and $P < .001$), GC with low TNM stage ($P < .001$ and $P < .001$), and EGC ($P < .001$ and $P < .001$),

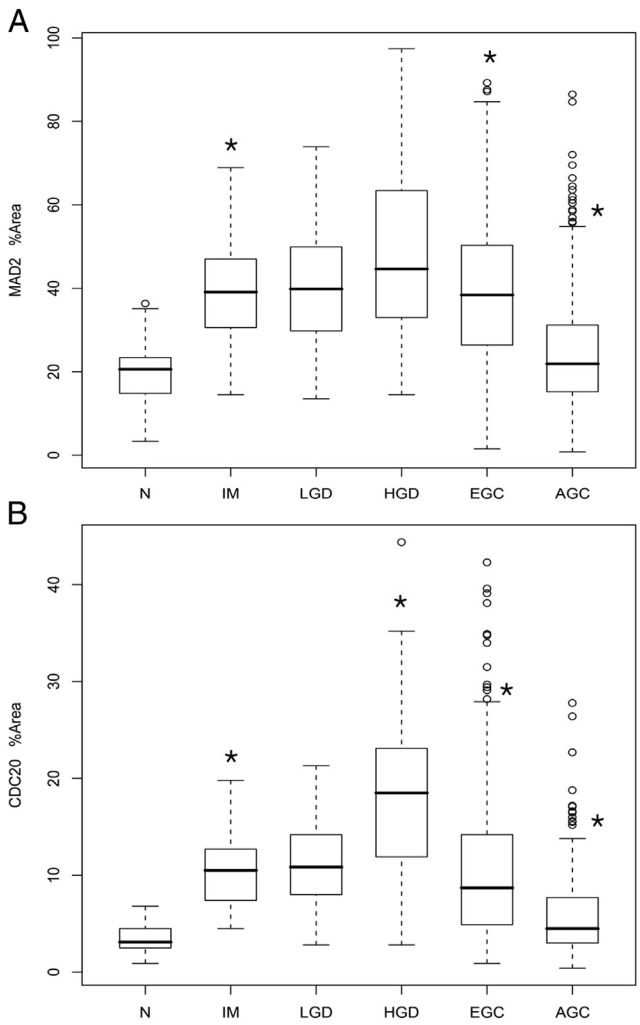

Fig. 1 Expression of MAD2 and CDC20 in normal, premalignant, and malignant gastric tissues. A, MAD2 is much more expressed in IM, LGD, HGD, and EGC than in normal gastric mucosa (N). MAD2 expression is the highest in HGD. B, CDC20 is much more expressed in IM, LGD, HGD, and EGC, compared with the N group. CDC20 expression is also the highest in HGD among these groups. Only significant *P* values are marked with an asterisk at the top of the graph bar when comparing between N and IM, IM and LGD, LGD and HGD, HGD and EGC, and EGC and AGC, respectively.

Table 2 Expression of MAD2 and CDC20 and CIC structures in early and advanced gastric adenocarcinomas

	Cases (n = 658)	MAD2 expression (%)			CDC20 expression (%)			CIC structures		
		Low (n = 320)	High (n = 338)	*P*	Low (n = 307)	High (n = 351)	*P*	Absent (n = 354)	Present n = 304)	*P*
Sex										
Male	436	192 (44.0)	244 (56.0)	.001 *	183 (42.0)	253 (58.0)	.001 *	224 (51.4)	212 (48.6)	.081
Female	222	128 (57.7)	94 (42.3)		124 (55.9)	98 (44.1)		130 (58.6)	92 (41.4)	
Age (y)										
<60	306	176 (57.5)	130 (42.5)	<.001 *	182 (59.5)	124 (40.5)	<.001 *	196 (64.1)	110 (35.9)	<.001 *
≥60	352	144 (40.9)	208 (59.1)		125 (35.5)	227 (64.5)		158 (44.9)	194 (55.1)	
Histologic type										
Intestinal	449	166 (37.0)	283 (63.0)	<.001 *	164 (36.5)	285 (63.5)	<.001 *	191 (42.5)	258 (57.5)	<.001 *
Diffuse	209	154 (73.7)	55 (26.3)		143 (68.4)	66 (31.6)		163 (78.0)	46 (22.0)	
TNM stage										
I, II	461	182 (39.5)	279 (60.5)	<.001 *	180 (39.0)	281 (61.0)	<.001 *	209 (45.3)	252 (54.7)	<.001 *
III, IV	197	138 (70.1)	59 (29.9)		127 (64.5)	70 (35.5)		145 (73.6)	52 (26.5)	
Invasion depth										
pT1a-T1b	345	100 (29.0)	245 (71.0)	<.001 *	108 (31.3)	237 (68.7)	<.001 *	140 (40.5)	205 (59.4)	<.001 *
pT2-T4	313	220 (70.3)	93 (29.7)		199 (63.6)	114 (36.4)		214 (68.4)	99 (31.6)	
Nodal status [a]										
pN0	310	119 (38.4)	191 (61.6)	<.001 *	123 (39.7)	187 (60.3)	<.001 *	147 (47.4)	163 (52.6)	<.001 *
pN1-N3	306	199 (65.0)	107 (35.0)		183 (59.8)	123 (40.2)		202 (66.0)	104 (34.0)	
ND [b]	42	2 (4.8)	40 (95.2)		1 (2.4)	41 (97.6)		5 (11.9)	37 (88.1)	
Distant metastasis										
Absent	635	303 (47.7)	332 (52.3)	.024 *	290 (45.7)	345 (54.3)	.014 *	333 (52.4)	302 (47.6)	<.001 *
Present	23	17 (73.9)	6 (26.1)		17 (73.9)	6 (26.1)		21 (91.3)	2 (8.7)	
Lymphatic invasion										
Absent	425	181 (42.6)	244 (57.4)	<.001 *	177 (41.7)	248 (58.3)	<.001 *	215 (50.6)	210 (49.4)	.032 *
Present	233	139 (59.7)	94 (40.3)		130 (55.8)	103 (44.2)		139 (59.7)	94 (40.3)	
Perineural invasion										
Absent	599	272 (45.4)	327 (54.6)	<.001 *	263 (43.9)	336 (56.1)	<.001 *	309 (51.6)	290 (48.4)	<.001 *
Present	59	48 (81.4)	11 (18.6)		44 (74.6)	15 (25.4)		45 (76.3)	14 (23.7)	
Recurrence										
No recurrence	527	225 (42.7)	302 (57.3)	<.001 *	223 (42.3)	304 (57.7)	<.001 *	260 (49.3)	267 (50.7)	<.001 *
Recurrence	131	95 (72.5)	36 (27.5)		84 (64.1)	47 (35.9)		94 (71.8)	37 (28.2)	

Abbreviation: ND, not dissected.

[a] Only the 2 groups with pN0 and pN1-N3, except the group with ND, were compared by χ^2 test.

[b] Lymph nodes were not dissected because the patients had undergone endoscopic submucosal dissection procedure.

* Statistically significant.

respectively. Overexpression of MAD2 and CDC20 also showed low frequencies of lymph node metastasis ($P < .001$ and $P < .001$, respectively), distant metastasis ($P = .024$ and $P = .014$), lymphatic invasion ($P < .001$ and $P < .001$), perineural invasion ($P < .001$ and $P < .001$, respectively), and tumor recurrence ($P < .001$ and $P < .001$).

In univariate survival analyses of all GC patients, high MAD2 and CDC20 expressions correlated with longer RFS ($P < .001$ and $P < .001$, respectively; Fig. 2A and B) and CSS ($P < .001$ and $P < .001$; Fig. 2C and D). On the other hand, shortened RFS and CSS were associated with diffuse histologic type ($P = .008$ and $P < .001$), lymphatic invasion ($P < .001$ and $P < .001$), perineural invasion ($P < .001$ and $P < .001$), and tumor presence at the resection margin ($P < .001$ and $P = .007$). In addition, shortened RFS was also related to advanced TNM stage ($P < .001$), and worse CSS was related to tumor recurrence ($P < .001$).

In multivariate analyses of all GC patients, high MAD2 expression was independently associated with longer RFS (hazard ratio [HR], 0.610; 95% confidence interval [CI], 0.415-0.899; $P = .012$), whereas CDC20 overexpression was related to longer CSS (HR, 0.634; 95% CI, 0.048-0.985; $P = .043$; Table 3). Poor prognostic factor for RFS was high TNM stage (HR, 4.607; 95% CI, 3.624-5.857; $P < .001$). Worse prognostic factors for CSS were high TNM stage (HR, 2.061; 95% CI, 1.541-2.757; $P < .001$) and tumor recurrence (HR, 7.778; 95% CI, 4.309-13.161; $P < .001$).

In multivariate analyses only in patients with AGC, high CDC20 expression was associated with favorable CSS (HR, 0.591; 95% CI, 0.362-0.965; $P = .036$). Poor prognostic factors for RFS were high TNM stage (HR, 3.137, 95% CI, 2.267-4.431; $P < .001$) and diffuse histologic type (HR, 1.463, 95% CI, 1.025-2.089, $P = .036$). Worse prognostic factors for CSS were advanced TNM stage (HR, 2.073; 95%

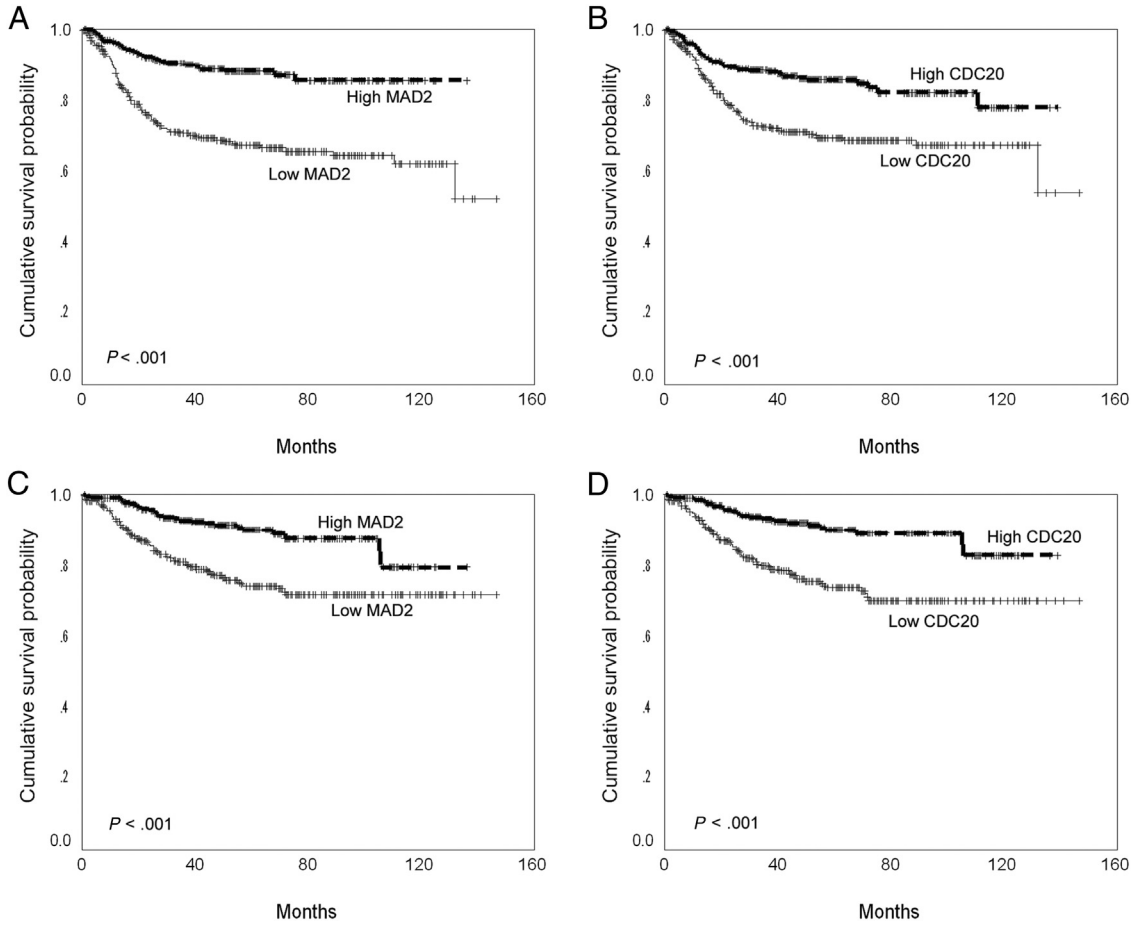

Fig. 2 Kaplan-Meier survival analysis of GC patients according to MAD2 and CDC20 expression. A and B, Patients with high levels of MAD2 and CDC20 expression have better RFS rates than did those with low MAD2 and CDC20 expression, respectively (log-rank test, $P < .001$ and $P < .001$). C and D, Patients with high levels of MAD2 and CDC20 expression have longer CSS rates than did those with low MAD2 and CDC20 expression, respectively (log-rank test, $P < .001$ and $P < .001$).

Table 3 Prognostic factors affecting RFS and CSS by multivariate analysis

	Variable	Factor	HR (95% CI)	*P*
EGC and AGC	RFS			
	TNM stage	High	4.607 (3.624-5.857)	<.001 *
	MAD2	Overexpression	0.610 (0.415-0.899)	.012 *
	CSS			
	TNM stage	High	2.061 (1.541-2.757)	<.001 *
	Recurrence	Present	7.778 (4.309-13.161)	<.001 *
	CDC20	Overexpression	0.634 (0.048-0.985)	.043 *
AGC only	RFS			
	TNM stage	High	3.137 (2.267-4.431)	<.001 *
	Histologic type	Diffuse	1.463 (1.025-2.089)	.036 *
	CSS			
	TNM stage	High	2.073 (1.402-3.066)	<.001 *
	Recurrence	Present	7.408 (4.241-12.939)	<.001 *
	CDC20	Overexpression	0.591 (0.362-0.965)	.036 *

* Statistically significant.

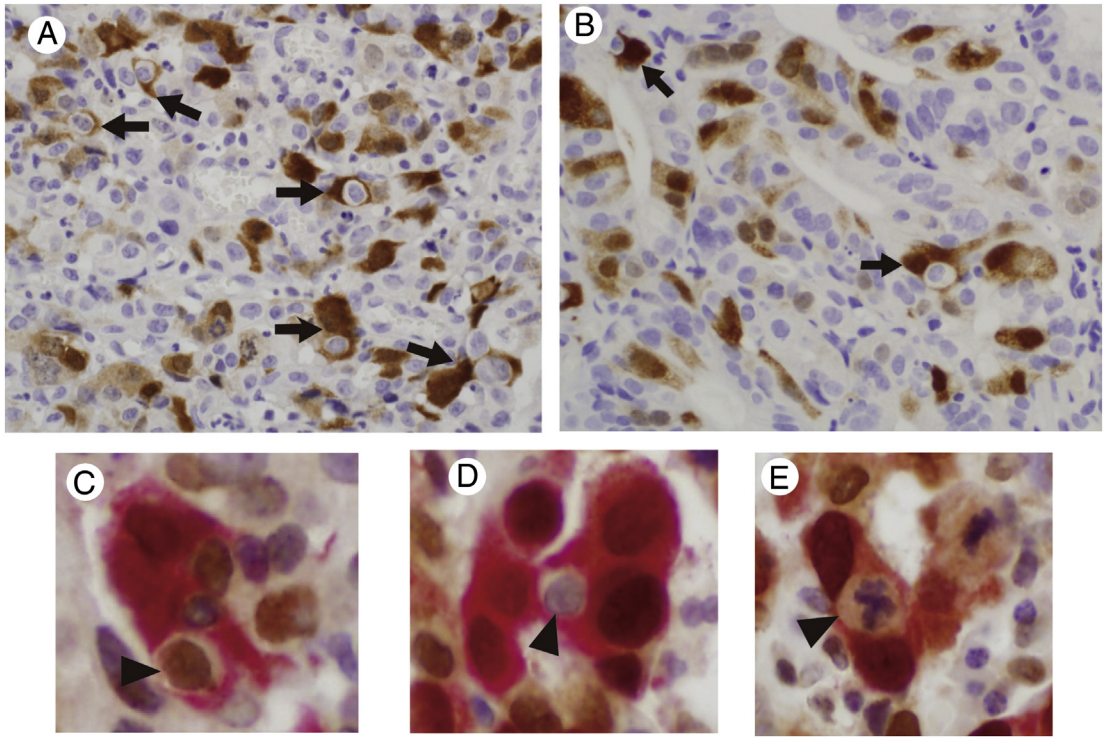

Fig. 3 Immunohistochemistry for CDC20 and double immunohistochemistry for MAD2 and CDC20. A, CDC20 immunostaining highlights the outer host cells (brown color, arrows) in CIC structures. B, In high-grade gastric dysplasia, CDC20-positive outer cells (brown color, arrows) encircle homotypic CDC20-negative inner cancer cells. C, On double staining for MAD2 (brown color) and CDC20 (red color), the outer cells express both MAD2 and CDC20, whereas the inner cancer cells (arrowhead) express MAD2. D, In addition, MAD2-negative inner cells (arrowhead) are surrounded by several CDC20-postive outer cells. E, Two cancer cells with coexpression of MAD2 and CDC20 encircle a cancer cell undergoing atypical mitosis (arrowhead). A-E, Original magnification ×400.

CI, 1.402-3.066; $P < .001$) and tumor recurrence (HR, 7.408, 95% CI, 4.241-12.939; $P < .001$).

3.2. CIC structures

Using immunohistochemistry for CDC20, CIC structures were easily highlighted in gastric dysplasia and GC lesions (Fig. 3). Specifically, almost all outer host cells in CIC formation strongly expressed CDC20, whereas the internalized tumor cells did not express CDC20 at all (Fig. 3A and B) In contrast, MAD2 was randomly expressed in tumor cells with or without CIC structures. Notably, the outer host cells expressed both MAD2 and CDC20. Unlike the immunostaining results of CDC20, MAD2 was either expressed or not expressed in the internalized cells (Fig. 3C and D). The internalized cells showing mitosis were occasionally observed (Fig. 3E). The outer host tumor cells engulfed not only neighboring homotypic tumor cells but also cells undergoing apoptosis and heterotypic immune cells including histiocytes, lymphocytes, and neutrophils (Supplementary Fig. 4).

CIC structures were occasionally found in IM (2/50; 4.0%) and LGD (7/50; 14.0%). In HGD, the frequency of CIC formation was abruptly increased (27/50; 54.0%). CIC structures was most frequently observed in EGC (205/345; 59.4%) and slightly decreased in AGC (99/313; 31.6%; Table 1). The mean number of CIC structures per high-power field was the highest in EGC among the gastric lesions (Fig. 4).

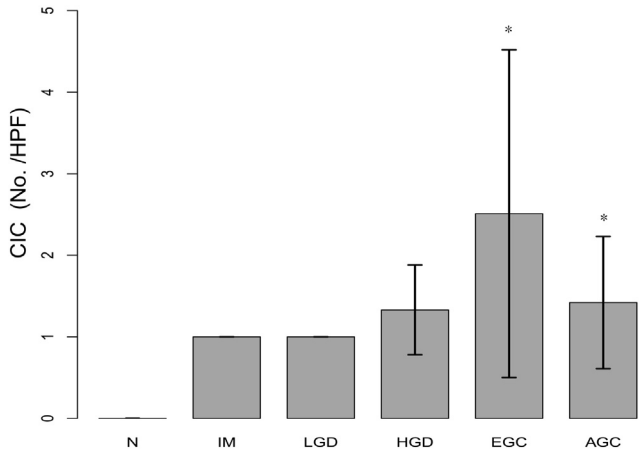

Fig. 4 The average number of homotypic CIC structures per high-power field is the most frequent in EGC and more common than the AGC group. CIC is not seen in normal gastric mucosa (N) lesion. Only significant *P* values are marked with an asterisk at the top of the graph bar when comparing between IM and LGD, LGD and HGD, HGD and EGC, and EGC and AGC, respectively.

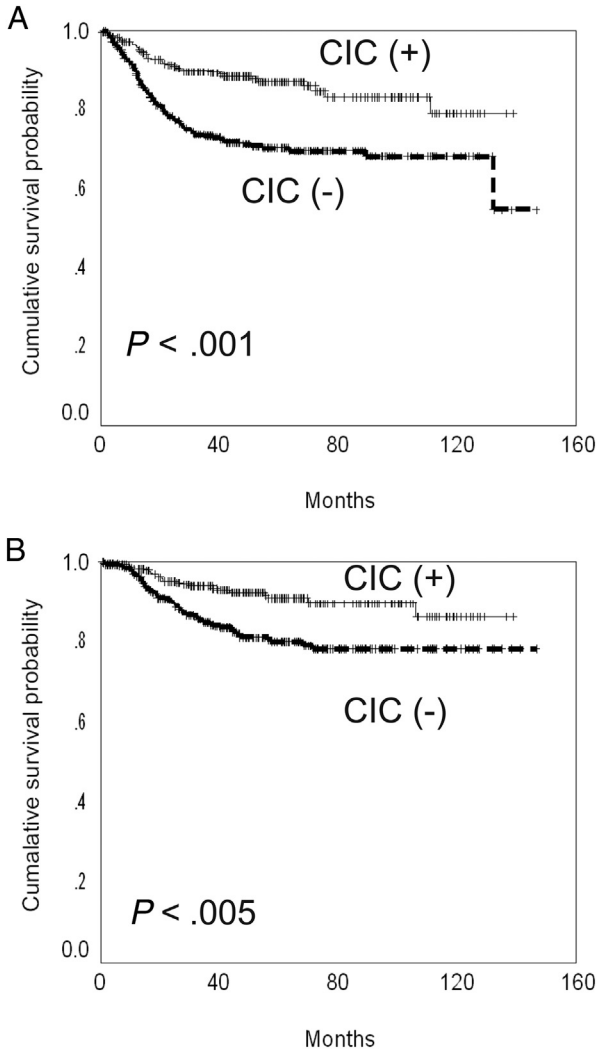

Fig. 5 GC patients with CIC structures show better RFS (A) and CSS (B) than those without CIC formation, respectively.

In EGC and AGC, CIC formation was associated with the intestinal type ($P < .001$), a lesser degree of invasiveness (T1 versus T2 or more, $P < .001$), and lower TNM stage (TNM I-II versus III-IV, $P < .001$). CIC structures were frequently observed in patients without lymphatic and/or distant metastases. CIC structures were inversely associated with perineural and lymphatic invasion or lymph node and distant metastases. (Table 2). In Kaplan-Meier survival analyses, CIC formation was associated with longer RFS ($P < .001$) and CSS ($P = .005$; Fig. 5A and B). However, CIC formation was not a statistically significant prognostic factor for RFS or CSS in multivariate survival analysis (Table 3).

4. Discussion

In this study, we found that the expression of MAD2 and CDC20, major components of SAC, was significantly increased in the premalignant and malignant gastric lesions, including IM, LGD, HGD, and EGC than in normal gastric mucosa. Their expression levels were highest in HGD. Intriguingly, CDC20 overexpression accentuates the outer cancer cells of CIC structures throughout the premalignant and malignant gastric lesions.

This study demonstrates that MAD2 and CDC20 are overexpressed in the premalignant and early stage of malignant lesions with the highest expression in the HGD, whereas their overexpressions in GC are closely associated with favorable clinicopathological factors, including intestinal histology, lower TNM stage, and longer RFS and CSS. These results are in agreement with previous studies [12,16] that GC tissues are more expressed than normal mucosa, but the fact that overexpression of MAD2 and CDC20 is related to poor prognostic factors is contrary to our results. Previous studies reported that MAD2 overexpression was associated with poorly differentiated histology and regional lymph node metastasis [16], whereas CDC20 was associated with increased tumor size, poor differentiation, lymph node involvement, higher TNM stage, and poor overall survival [12]. More recently, however, comprehensive gene expression and subsequent clinicopathological studies have proposed 4 molecular subtypes of GC, among which CIN subtype is characterized by intestinal histology, *TP53* mutations, and a high frequency of aneuploidy, and has a better prognosis than that of microsatellite instable or genomically stable subtypes [7,23]. Thus, given that overexpression of MAD2 and CDC20 induces CIN and aneuploidy and is associated with intestinal histology and *TP53* mutations [24], it is possible that GC patients with MAD2 or CDC20 overexpression could be classified into the CIN subtype, which has better survival outcomes than other molecular subtypes [23].

Furthermore, it was reported that MAD2 overexpression is needed for tumor initiation, but not for tumor maintenance in transgenic mice [25]. This pattern of MAD2 overexpression, which suggests a crucial role in the early stages of carcinogenesis, has also been reported in the premalignant and malignant squamous lesions of the human uterine cervix [15] and in the metaplastic and dysplastic lesions and adenocarcinomas arising from the Barrett esophagus [13]. In addition, our results showed that MAD2 and CDC20 overexpressions were sharply reduced in the invasive fronts of EGC compared with the adjacent HGD. The expression pattern of MAD2 and CDC20 in the precancerous and malignant gastric lesions may remind us of their potential expressions in GC stem cells. During gastric carcinogenesis, particularly in metaplasia and dysplasia, stem cells and their niche at the proliferative gastric isthmic region are activated and expanded in response to tissue injury and inflammation. Indeed, it is known that overexpression of MAD2 and CDC20 increases nasopharyngeal stem cells and is required for the survival of glioblastoma stem cells, respectively [26,27]. However, further studies are needed to prove this possibility. Taken together, it is suggested that MAD2 and CDC20 overexpressions play important roles in the early phase of gastric carcinogenesis, rather than in cancer progression.

Because the roles of MAD2 and CDC20 in SAC are somewhat different, overexpression of MAD2 and CDC20 differ in the mechanisms of CIN and aneuploidy induction. MAD2, a key component of mitotic checkpoint complex, inhibits the functions of APC/C and its overexpression can delay the entry into anaphase, whereas CDC20 is a dual player that inhibits or activates APC/C. In normal cells, MAD2 overexpression causes TP53-dependent G1 arrest or mitotic cell death due to prolonged mitosis, but MAD2-overexpressing cancer cells are so well tolerated because overexpressed TRIP13 and p31^{comet} oppose the effects of MAD2 overexpression [28]. Premalignant and malignant gastric lesions show increased *TP53* mutations and Rb alterations, particularly in the early stage of GC development [29,30]. The *TP53* mutations and Rb-E2F pathway deregulation lead to the overexpression of MAD2 and CDC20 [8-10]. MAD2 overexpression promotes hyperstabilization of kinetochore-microtubule attachments, resulting in lagging chromosomes, aneuploidy formation in vitro [31], and tumor initiation through the acquisition of a CIN phenotype in transgenic mice [25]. CDC20 overexpression induces premature anaphase entry, CIN, and aneuploidy by forming a complex with APC/C-CBP/p300-E2F1/DP1 and subsequent activating UBCH10 promoter through the E2F1 binding site [9]. However, further studies are needed to determine whether MAD2 and CDC20 overexpressions induce CIN and aneuploidy during gastric carcinogenesis.

It is noteworthy that CDC20 immunohistochemistry strongly stains the external host cells of CIC formation surrounding the adjacent inner cancer cells in tissue sections. The CIC formation by cell cannibalism, entosis, or emperitosis has been reported in a variety of carcinomas [32]. The CIC phenomenon has been suggested as a way to gain energy for cancer cell proliferation and survival from starvation or unfavorable microenvironment [33]. Although the CIC is made by any process such as entosis, cell cannibalism, or emperitosis, ultimately the outer host cancer cells will have CIN and aneuploidy in common. This is probably due to the process of cytokinesis failure, cell fusion, or direct exchange of genetic material [19]. In fact, it is very difficult to distinguish cell cannibalism from entosis or emperitosis because some proteins are commonly participated in these processes. For instance, transmembrane protein TM9SF4 and pH-dependent proteases are considered key molecules for cancer cell cannibalism [34]. However, Rho and Rho kinases, major players in entosis, might be also involved in cancer cell cannibalism [35]. In the present study, CIC structures are more frequently observed in EGC and intestinal type AGC, where CIN phenotype and aneuploidy are more frequent than other gastric lesions [7]. Furthermore, CIC formation was mostly associated with favorable prognostic parameters. The clinicopathological significances of CIC structures remain controversial because this phenomenon has been suggested to function as an oncosupressor [32] or to promote tumor progression [18,19]. A recent study revealed that cancer cells engulfing mesenchymal stromal/stem cells were associated with tumor dormancy and suppressed tumorigenicity rather than cancer cell proliferation [35]. Taken together, the specific expression of CDC20 in the outer host cells of CIC formation might reflect the status of CIN and aneuploidy [19]. The CIC formation may play roles in the early stage of GC development, like the SAC protein overexpressions, but not in the progression or metastasis of cancer cells. However, to understand the clinicopathological implications of CIC formation, further studies are needed.

In conclusion, this study demonstrates that MAD2 and CDC20 are the most highly expressed in the precancerous HGD lesion, and CIC structures are the most frequently found in EGC, suggesting that the SAC proteins and CIC formation participate in the initiation or early stage of GC development. Because the overexpression of MAD2 and CDC20 in GC is closely associated with intestinal histology type and favorable clinicopathological factors, as well as CIN, this might be helpful to separate CIN-type GC immunohistochemically from other molecular subtypes. Moreover, the host cancer cells of the CIC structures are distinguished from other cancer cells very easily by CDC20 immunohistochemical staining.

Supplementary data

Supplementary data to this article can be found online at https://doi.org/10.1016/j.humpath.2018.10.029.

References

[1] Fitzmaurice C, Dicker D, Pain A, et al. The global burden of cancer 2013. JAMA Oncol 2015;1:505-27.
[2] Figueiredo C, Camargo MC, Leite M, et al. Pathogenesis of gastric cancer: genetics and molecular classification. Curr Top Microbiol Immunol 2017;400:277-304.
[3] Schukken KM, Foijer F. CIN and aneuploidy: different concepts, different consequences. Bioessays 2018;40.
[4] Lau DT, Murray AW. Mad2 and Mad3 cooperate to arrest budding yeast in mitosis. Curr Biol 2012;22:180-90.
[5] Hoyt MA, Totis L, Roberts BT. *S. cerevisiae* genes required for cell cycle arrest in response to loss of microtubule function. Cell 1991;66:507-17.
[6] De Antoni A, Pearson CG, Cimini D, et al. The Mad1/Mad2 complex as a template for Mad2 activation in the spindle assembly checkpoint. Curr Biol 2005;15:214-25.
[7] Cancer Genome Atlas Research Network. Comprehensive molecular characterization of gastric adenocarcinoma. Nature 2014;513:202-9.
[8] Hernando E, Nahle Z, Juan G, et al. Rb inactivation promotes genomic instability by uncoupling cell cycle progression from mitotic control. Nature 2004;430:797-802.
[9] Nath S, Chowdhury A, Dey S, et al. Deregulation of Rb-E2F1 axis causes chromosomal instability by engaging the transactivation function of Cdc20-anaphase–promoting complex/cyclosome. Mol Cell Biol 2015;35:356-69.
[10] Schvartzman JM, Duijf PHG, Sotillo R, Coker C, Benezra R. Mad2 is a critical mediator of the chromosome instability observed upon Rb and p53 pathway inhibition. Cancer Cell 2011;19:701-14.
[11] Simonetti G, Bruno S, Padella A, Tenti E, Martinelli G. Aneuploidy: cancer strength or vulnerability? Int J Cancer 2018;144:8-25.

[12] Ding ZY, Wu HR, Zhang JM, Huang GR, Ji DD. Expression characteristics of CDC20 in gastric cancer and its correlation with poor prognosis. Int J Clin Exp Pathol 2014;7:722-7.
[13] Doak SH, Jenkins GJ, Parry EM, et al. Differential expression of the MAD2, BUB1 and HSP27 genes in Barrett's oesophagus—their association with aneuploidy and neoplastic progression. Mutat Res 2004;547:133-44.
[14] Furlong F, Fitzpatrick P, O'Toole S, et al. Low MAD2 expression levels associate with reduced progression-free survival in patients with high-grade serous epithelial ovarian cancer. J Pathol 2012;226:746-55.
[15] Kim Y, Choi JW, Lee JH, Kim YS. MAD2 and CDC20 are upregulated in high-grade squamous intraepithelial lesions and squamous cell carcinomas of the uterine cervix. Int J Gynecol Pathol 2014;33:517-23.
[16] Wang L, Yin F, Du Y, et al. MAD2 as a key component of mitotic checkpoint: a probable prognostic factor for gastric cancer. Am J Clin Pathol 2009;131:793-801.
[17] Yang YQ, Li JC. Progress of research in cell-in-cell phenomena. Anat Rec (Hoboken) 2012;295:372-7.
[18] He MF, Wang S, Wang Y, Wang XN. Modeling cell-in-cell structure into its biological significance. Cell Death Dis 2013;4:e630.
[19] Krajcovic M, Overholtzer M. Mechanisms of ploidy increase in human cancers: a new role for cell cannibalism. Cancer Res 2012;72:1596-601.
[20] Amin MB, Edge S, Greene F, et al, editors. AJCC Cancer Staging Manual. Springer International Publishing; 2017.
[21] Ilyas M, Grabsch H, Ellis IO, et al. Guidelines and considerations for conducting experiments using tissue microarrays. Histopathology 2013;62:827-39.
[22] Zlobec I, Steele R, Terracciano L, Jass JR, Lugli A. Selecting immunohistochemical cut-off scores for novel biomarkers of progression and survival in colorectal cancer. J Clin Pathol 2007;60:1112-6.
[23] Sohn BH, Hwang JE, Jang HJ, et al. Clinical significance of four molecular subtypes of gastric cancer identified by the cancer genome atlas project. Clin Cancer Res 2017;23:4441-9.
[24] Maleki SS, Rocken C. Chromosomal instability in gastric cancer biology. Neoplasia 2017;19:412-20.
[25] Sotillo R, Hernando E, Diaz-Rodriguez E, et al. Mad2 overexpression promotes aneuploidy and tumorigenesis in mice. Cancer Cell 2007;11:9-23.
[26] Liang Y, Zhong Z, Huang Y, et al. Stem-like cancer cells are inducible by increasing genomic instability in cancer cells. J Biol Chem 2010;285:4931-40.
[27] Mao DD, Gujar AD, Mahlokozera T, et al. A CDC20-APC/SOX2 signaling axis regulates human glioblastoma stem–like cells. Cell Rep 2015;11:1809-21.
[28] Marks DH, Thomas R, Chin Y, et al. Mad2 overexpression uncovers a critical role for TRIP13 in mitotic exit. Cell Rep 2017;19:1832-45.
[29] Yakirevich E, Resnick MB. Pathology of gastric cancer and its precursor lesions. Gastroenterol Clin North Am 2013;42:261-84.
[30] Abdel-Aziz A, Ahmed RA, Ibrahiem AT. Expression of pRb, Ki67 and HER 2/neu in gastric carcinomas: relation to different histopathological grades and stages. Ann Diagn Pathol 2017;30:1-7.
[31] Kabeche L, Compton DA. Checkpoint-independent stabilization of kinetochore-microtubule attachments by Mad2 in human cells. Curr Biol 2012;22:638-44.
[32] Overholtzer M, Mailleux AA, Mouneimne G, et al. A nonapoptotic cell death process, entosis, that occurs by cell-in-cell invasion. Cell 2007;131:966-79.
[33] Fais S. Cannibalism: a way to feed on metastatic tumors. Cancer Lett 2007;258:155-64.
[34] Foley EA, Kapoor TM. Microtubule attachment and spindle assembly checkpoint signalling at the kinetochore. Nat Rev Mol Cell Biol 2013;14:25-37.
[35] Bartosh TJ, Ullah M, Zeitouni S, Beaver J, Prockop DJ. Cancer cells enter dormancy after cannibalizing mesenchymal stem/stromal cells (MSCs). Proc Natl Acad Sci U S A 2016;113:E6447-56.